International Journal of Thermophysics, Vol. 19, No. 4, 1998

Molecular Dynamics Calculation of the Viscosities of Biaxial Nematic Liquid Crystals[1]

S. Sarman[2]

We have evaluated the Green–Kubo relations for the viscosities of a biaxial nematic liquid crystal by performing equilibrium molecular dynamics simulations. The viscosity varies by more than two orders of magnitude depending on the orientation of the directors relative to the streamlines. The molecules consist of nine fused Gay–Berne oblates whose axes of revolution are parallel to each other and perpendicular to the line joining their centers of mass. This gives a biaxial body, the length-to-width-to-breadth ratio of which is equal to 5:1:0.4. The numerical evaluation of the Green–Kubo relations for the viscosities is facilitated by the application of a Gaussian director constraint algorithm that makes it possible to fix the directors in space. This does not only generate an inertial director-based frame but also a new equilibrium ensemble. In this ensemble the Green–Kubo relations for the viscosities are simple linear combinations of time correlation function integrals, whereas they are complicated rational functions in the conventional canonical ensemble.

KEY WORDS: biaxial nematic liquid crystals; director constraint algorithms; Gay–Berne potentials; Green–Kubo relations; molecular dynamics simulations; viscosities.

1. INTRODUCTION

Transport phenomena in liquid crystals are much richer than in isotropic fluids. The reason for this is that the lower symmetry of the liquid crystals allows cross-couplings between thermodynamic forces and fluxes that are forbidden in isotropic fluids. The diffusion coefficients and the thermal conductivities are second-rank tensors with two or three independent components depending on whether the symmetry is unaxial or biaxial. The viscosity is a fourth-rank tensor with 81 independent components in the

[1] Paper presented at the Thirteenth Symposium on Thermophysical Properties, June 22–27, 1997, Boulder, Colorado, U.S.A.

[2] Institutionen för Fysikalisk Kemi, Göteborgs Universitet, S-412 96 Göteborg, Sweden.

0195-928X/98/0700-1073$15.00/0

general case. In an isotropic fluid there are three independent components: the shear viscosity, the volume viscosity, and the vortex viscosity. In uniaxial systems there are 7 viscosities, and in biaxial systems there are 15. There are cross-couplings between tensors of different rank and parity. For example, the symmetric traceless strain rate cross-couples with the antisymmetric pressure. This gives rise to director alignment phenomena in shear flows.

The first evaluation of the viscosities of a liquid crystal model system was done by Baalss and Hess [1]. They performed a shear-flow simulation of a perfectly aligned nematic liquid crystal. In order to decrease the computational work they devised a mapping of the liquid crystal onto an isotropic Lennard–Jones fluid. Equilibrium fluctuation relations for the viscosities of uniaxial nematic liquid crystals were first derived by Forster [2] using projector operator techniques. The same relations were later derived by Sarman and Evans [3] by applying the SLLOD equations of motion for planar Couette flow and linear response theory. These relations were evaluated numerically for the Gay–Berne fluid [4]. In a later work we devised a Gaussian constraint algorithm that made it possible to fix the director in space [5]. This makes a director-based frame an inertial frame. One also generates a new equilibrium ensemble. It turns out that the Green–Kubo relations for the various viscosity coefficients are linear combinations of time correlation function integrals in this ensemble, whereas they are complicated rational functions in the conventional canonical ensemble. The Green–Kubo relations for the various viscosity coefficients have recently been generalized to biaxial nematic liquid crystals [6]. In this work we apply these relations to a model fluid consisting of molecules composed of nine Gay–Berne oblates [7]. Their axes of revolution are parallel to each other and perpendicular to the line joining their centers of mass. The length-to-width-to-breadth ratio is 5:1:0.4. This system has been shown to form biaxial nematic phases at high densities.

2. THEORY

The degree of ordering in a biaxial liquid crystal is described by two second-rank order parameters [8, 9]:

$$Q^2_{00} \equiv \langle \tfrac{1}{2}(3\cos^2\theta - 1)\rangle \tag{1}$$

$$Q^2_{22} \equiv \langle \tfrac{1}{2}(1+\cos^2\theta)\cos 2\phi \cos 2\psi - \cos\theta \sin 2\phi \sin 2\psi\rangle \tag{2}$$

where θ, ϕ, and ψ are the Euler angles relative to a laboratory-based coordinate system. The first parameter is the well-known uniaxial order parameter. It is zero in isotropic phases and finite in uniaxially or biaxially

symmetric phases. The other parameter is the biaxial order parameter. It is zero in isotropic and uniaxial phases, and it is finite in biaxial phases. The order parameters can be defined more clearly if we form symmetric traceless order tensors based on the various principal molecular axes,

$$\mathbf{Q}^{ss} \equiv \frac{3}{2}\left(\frac{1}{N}\sum_{i=1}^{N}\hat{\mathbf{s}}_i\hat{\mathbf{s}}_i - \frac{1}{3}\mathbf{1}\right) \tag{3}$$

where N is the number of particles, $\mathbf{1}$ is the unit second-rank tensor, and $\hat{\mathbf{s}}_i$ is one of the principal axes $\hat{\mathbf{u}}_i$, $\hat{\mathbf{v}}_i$ or $\hat{\boldsymbol{w}}_i$ of the molecule (see Fig. 1). This gives three order tensors, $\mathbf{Q}^{uu}$, $\mathbf{Q}^{vv}$, and $\mathbf{Q}^{ww}$. Using these definitions the order parameters can be rewritten as

$$Q_{00}^2 = \langle \mathbf{e}_z \cdot \mathbf{Q}^{ww} \cdot \mathbf{e}_z \rangle \tag{4}$$

and

$$Q_{22}^2 = \tfrac{1}{3}\langle \mathbf{e}_x \cdot \mathbf{Q}^{uu} \cdot \mathbf{e}_x + \mathbf{e}_y \cdot \mathbf{Q}^{vv} \cdot \mathbf{e}_y - \mathbf{e}_y \cdot \mathbf{Q}^{uu} \cdot \mathbf{e}_y - \mathbf{e}_x \cdot \mathbf{Q}^{vv} \cdot \mathbf{e}_x \rangle \tag{5}$$

where $(\mathbf{e}_x, \mathbf{e}_y, \mathbf{e}_z)$ is the base of a laboratory-based coordinate system. The parameter Q_{00}^2 is the largest eigenvalue of the order tensor $\mathbf{Q}^{ww}$.

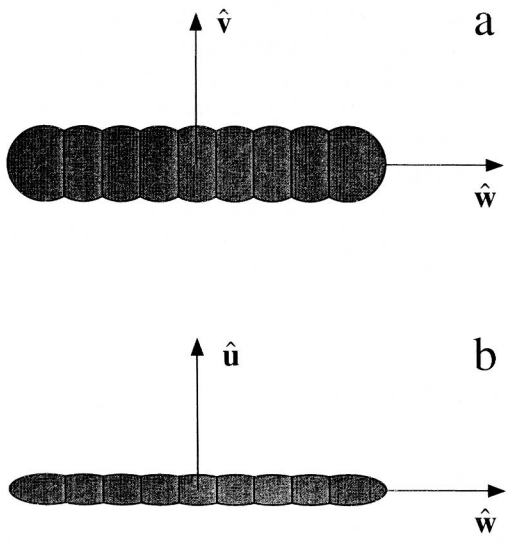

Fig. 1. Planar projections of the molecular model. (a) The $\hat{\mathbf{u}}$-axis is perpendicular to the plane of the paper. (b) The $\hat{\mathbf{v}}$-axis is perpendicular to the plane of the paper.

In order to make sense of these order parameters we have to define the coordinate system. This can be done by calculating the three order tensors $\mathbf{Q}^{uu}$, $\mathbf{Q}^{vv}$, and $\mathbf{Q}^{ww}$. Then one computes the largest eigenvalue of each of them. One defines the eigenvector pertaining to the largest of these eigenvalues, $\mathbf{n}_1$, as the x-direction. The eigenvector corresponding to the second largest eigenvalue, $\mathbf{n}_2$, is defined as the y-direction. The z-direction is given by $\mathbf{n}_3$, which is the eigenvector corresponding to the smallest eigenvalue. In a small system such as a simulation cell, these eigenvectors are independent within certain limits and they are not strictly orthogoanl. They are constantly diffusing on the unit sphere at angular velocities defined as $\boldsymbol{\Omega}_\mu = \mathbf{n}_\mu \times \dot{\mathbf{n}}_\mu$, $\mu = 1, 2, 3$. This problem can be solved by applying a Gaussian constraint algorithm, described below, to fix the directors and keep them orthogonal.

We are going to use a model system consisting of rigid bodies. The equations of motion for such a system are

$$\dot{\mathbf{q}}_i = \frac{\mathbf{p}_i}{M} \tag{6}$$

and

$$\dot{\mathbf{p}}_i = \mathbf{F}_i - \alpha \mathbf{p}_i \tag{7}$$

where

$$\alpha = \sum_{i=1}^{N} \mathbf{p}_i \cdot \mathbf{F}_i \Big/ \sum_{i=1}^{N} \mathbf{p}_i^2 \tag{8}$$

$\mathbf{q}_i$ and $\mathbf{p}_i$ are the position and the linear momentum of particle i, M is the molecular mass, and $\mathbf{F}_i$ is the force on particle i due to interactions with other particles. The parameter α is a Gaussian thermostatting multiplier that is determined in such a way that the translational kinetic energy becomes a constant of motion [10]. An important property of this thermostat is that it does not exert any torque on the system. Consequently, it does not interfere with the director alignment or rotation. In angular space we employ,

$$\dot{\hat{\mathbf{s}}} = \boldsymbol{\omega}_i \times \hat{\mathbf{s}}_i \tag{9}$$

and the Euler equations,

$$\mathbf{I}_p \cdot \dot{\boldsymbol{\omega}}_{pi} = -\boldsymbol{\omega}_{pi} \times \mathbf{I}_p \cdot \boldsymbol{\omega}_{pi} + \boldsymbol{\Gamma}_{pi} + \sum_{\mu=1}^{3} \lambda_\mu \cdot \frac{\partial \boldsymbol{\Omega}_\mu}{\partial \boldsymbol{\omega}_{pi}} \tag{10}$$

where

$$\mathbf{I}_p = \begin{pmatrix} \mathbf{I}_{puu} & 0 & 0 \\ 0 & \mathbf{I}_{pvv} & 0 \\ 0 & 0 & \mathbf{I}_{pww} \end{pmatrix}$$

is the inertia tensor, $\hat{\mathbf{s}}_i$ equals $\hat{\mathbf{u}}_i$, $\hat{\mathbf{v}}_i$, or $\hat{\mathbf{w}}_i$, the principal axes of molecule i, $\boldsymbol{\omega}_{pi}$ is the molecular angular velocity, $\boldsymbol{\Gamma}_{pi}$ is the torque due to interactions with other particles, and $\mathbf{I}_{p\alpha\alpha}$, $\alpha = u, v, w$, is the moment of inertia around the α-axis. Do not confuse the subscript "α" with the thermostatting multiplier α. The subscript "p" denotes the principal frame. The Gaussian constraint multiplier λ_μ keeps $\boldsymbol{\Omega}_\mu$ equal to zero and thereby the director orientations are fixed in space. The λ_μ's are determined by the requirements that

$$\dot{\boldsymbol{\Omega}}_\mu = \mathbf{0}, \qquad \mu = 1, 2, 3 \tag{11}$$

This is actually six independent equations because there are two independent components of each of the $\boldsymbol{\Omega}_\mu$'s and the λ_μ's. Provided that the initial values of the $\boldsymbol{\Omega}_\mu$'s are zero, they will remain zero at all times and the directors will remain fixed. When these constraints are applied, the system will evolve according to synthetic equations of motion. However, the system remains in equilibrium and it is possible to prove that the ensemble averages of most thermodynamic properties and time correlation functions are unchanged [11].

The $\alpha\beta$ element of the pressure tensor is denoted $p_{\alpha\beta}$. We employ the Irving–Kirkwood [12] definition of the pressure,

$$\langle \mathbf{P} \rangle V = \left\langle \sum_{i=1}^{N} \left[\frac{\mathbf{p}_i \mathbf{p}_i}{m} - \mathbf{r}_i \mathbf{F}_i \right] \right\rangle = \left\langle \sum_{i=1}^{N} \frac{\mathbf{p}_i \mathbf{p}_i}{m} - \sum_{i=1}^{N} \sum_{j>i} \mathbf{r}_{ij} \mathbf{F}_{ij} \right\rangle \tag{12}$$

where $\mathbf{r}_{ij} = \mathbf{r}_j - \mathbf{r}_i$ and $\mathbf{F}_{ij}$ is the force acting on particle i due to interactions with particle j.

3. MODEL SYSTEM AND TECHNICAL DETAILS

Our molecules consist of a string of Gay–Berne oblates [8] where the axes of revolution of the oblates are parallel to each other and perpendicular to the line joining their centers of mass. In order to decrease the number of interactions we replace the Lennard–Jones core by a purely repulsive $1/r^{18}$ core. The site–site interaction potential becomes

$$U(\mathbf{r}_{1\alpha 2\beta}, \hat{\mathbf{u}}_1, \hat{\mathbf{u}}_2) = 4\varepsilon(\hat{\mathbf{r}}_{1\alpha 2\beta}, \hat{\mathbf{u}}_1, \hat{\mathbf{u}}_2) \left[\frac{\sigma_0}{r_{1\alpha 2\beta} - \sigma(\hat{\mathbf{r}}_{1\alpha 2\beta}, \hat{\mathbf{u}}_1, \hat{\mathbf{u}}_2) + \sigma_0} \right]^{18} \tag{13}$$

where $\mathbf{r}_{1\alpha 2\beta}$ is the distance vector from the center of mass of interaction site α of molecule 1 to the center of mass of interaction site β of molecule 2, $\hat{\mathbf{r}}_{1\alpha 2\beta}$ is the unit vector in the direction of $\mathbf{r}_{1\alpha 2\beta}$, $r_{1\alpha 2\beta}$ is the length of $\mathbf{r}_{1\alpha 2\beta}$, and $\hat{\mathbf{u}}_1$ and $\hat{\mathbf{u}}_2$ are the unit vectors parallel to the axis of revolution of the oblates of molecules 1 and 2, respectively. The parameter σ_0 is the length of the major axis of the oblate. The strength and range parameters $\varepsilon(\hat{\mathbf{r}}_{1\alpha 2\beta}, \hat{\mathbf{u}}_1, \hat{\mathbf{u}}_2)$ and $\sigma(\hat{\mathbf{r}}_{1\alpha 2\beta}, \hat{\mathbf{u}}_1, \hat{\mathbf{u}}_2)$ are given by

$$\varepsilon(\hat{\mathbf{r}}_{1\alpha 2\beta}, \hat{\mathbf{u}}_1, \hat{\mathbf{u}}_2) = \varepsilon_0[1-\chi^2(\hat{\mathbf{u}}_1\cdot\hat{\mathbf{u}}_2)^2]^{-1/2} \cdot\left\{1-\frac{\chi'}{2}\left[\frac{(\hat{\mathbf{r}}_{1\alpha 2\beta}\cdot\hat{\mathbf{u}}_1+\hat{\mathbf{r}}_{1\alpha 2\beta}\cdot\hat{\mathbf{u}}_2)^2}{1+\chi'\hat{\mathbf{u}}_1\cdot\hat{\mathbf{u}}_2}+\frac{(\hat{\mathbf{r}}_{1\alpha 2\beta}\cdot\hat{\mathbf{u}}_1-\hat{\mathbf{r}}_{1\alpha 2\beta}\cdot\hat{\mathbf{u}}_2)^2}{1-\chi'\hat{\mathbf{u}}_1\cdot\hat{\mathbf{u}}_2}\right]\right\}^2 \tag{14}$$

and

$$\sigma(\hat{\mathbf{r}}_{1\alpha 2\beta}, \hat{\mathbf{u}}_1, \hat{\mathbf{u}}_2) = \sigma_0\left\{1-\frac{\chi}{2}\left[\frac{(\hat{\mathbf{r}}_{1\alpha 2\beta}\cdot\hat{\mathbf{u}}_1+\hat{\mathbf{r}}_{1\alpha 2\beta}\cdot\hat{\mathbf{u}}_2)^2}{1+\chi\hat{\mathbf{u}}_1\cdot\hat{\mathbf{u}}_2}+\frac{(\hat{\mathbf{r}}_{1\alpha 2\beta}\cdot\hat{\mathbf{u}}_1-\hat{\mathbf{r}}_{1\alpha 2\beta}\cdot\hat{\mathbf{u}}_2)^2}{1-\chi\hat{\mathbf{u}}_1\cdot\hat{\mathbf{u}}_2}\right]\right\}^{-1/2} \tag{15}$$

The parameter $\chi \equiv (\kappa^2-1)/(\kappa^2+1)$, where κ is the ratio of the axis of revolution and the axis perpendicular to the axis of revolution and $\chi' \equiv (\kappa'^{1/2}-1)/(\kappa'^{1/2}+1)$, where κ' is the ratio of the potential energy minima of the side-to-side and the end-to-end configurations. The depth of the potential minimum of the configuration where $\mathbf{r}_{1\alpha 2\beta}$, $\hat{\mathbf{u}}_1$, and $\hat{\mathbf{u}}_2$ are mutually perpendicular is given by ε_0. Note that we use purely repulsive potentials, so there are no potential minima. However, we keep the values of κ', χ', and ε_0 adjusted for a Lennard–Jones potential when we replace it by a purely repulsive potential in Eq. (13). The molecules consist of nine interaction sites. Their axis vectors $\hat{\mathbf{u}}_i$ are parallel to each other and perpendicular to the line joining the centers of mass. The distance between the centers of mass of the oblates is $\sigma_0/2$ (see Fig. 1). The parameters κ and κ' have been given the values 0.40 and 0.20, respectively. This gives a length-to-breadth-to-width ratio of 5:1:0.40. The numerical results in this work are expressed in units of σ_0, M, and $\sigma_0(M/\varepsilon_0)^{1/2}$. The moment of inertia around the $\hat{\mathbf{w}}_i$-axis is equal to $0.25M\sigma_0^2$. The moments of inertia around the $\hat{\mathbf{u}}_i$- and the $\hat{\mathbf{v}}_i$-axes are equal to $1.8M\sigma_0^2$. The equations of motion have been integrated by a fourth-order Gear predictor corrector with a time step of 0.001τ. The cutoff radius beyond which the interaction potential and the interaction forces are set equal to zero is $1.5\sigma(\hat{\mathbf{r}}_{1\alpha 2\beta}, \hat{\mathbf{u}}_1, \hat{\mathbf{u}}_2)$. Thus the cutoff radius is orientation dependent. The

expressions for the forces and the torques, which are rather complicated, are given in Ref. 13. We used cubic boundary conditions. We employed 2025 molecules which together contain 18,225 oblate Gay–Berne interaction sites. The length of the simulation was 9600τ. The error bars were obtained by dividing the simulation into four equal parts and calculating the standard deviation between the subaverages.

4. CALCULATIONS, RESULTS, AND DISCUSSION

We have evaluated the Miesowicz viscosities or the effective viscosities of our variant of the Gay–Berne fluid at a reduced density of 0.19 and a reduced temperature of 1.00. In a planar Couette flow, the relation between the pressure and the strain rate is

$$\langle p_{\alpha\beta} \rangle = -\eta_\gamma \frac{\partial u_\beta}{\partial r_\alpha} \tag{16}$$

where u_β is the velocity in the $\mathbf{n}_\beta$ direction that varies in the $\mathbf{n}_\alpha$ direction in a director-based coordinate system. The $\mathbf{n}_\gamma$ axis is perpendicular to the vorticity plane and the $\mathbf{n}_\alpha$ axis is perpendicular to the shear plane (see Fig. 2). Thus $\partial u_\beta / \partial r_\alpha$ is the strain rate, η_γ is the effective viscosity, and

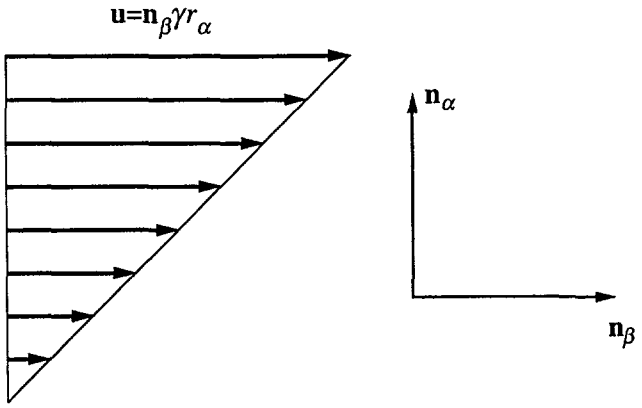

Fig. 2. A strain rate $\nabla \mathbf{u} = \gamma \mathbf{n}_\alpha \mathbf{n}_\beta$ is applied. The director $\mathbf{n}_\beta$ is parallel to the streamlines. The velocity varies in the $\mathbf{n}_\alpha$ direction which is perpendicular to the shear plane. The director $\mathbf{n}_\gamma$ is perpendicular to the vorticity plane and the plane of the paper. The axis parallel to this director has been omitted. We denote the effective viscosity η_γ if $\{\alpha, \beta, \gamma\}$ is an even permutation of $\{1, 2, 3\}$ and $\eta_{-\gamma}$ for odd permutations.

$\langle p_{\alpha\beta} \rangle$ is the $\alpha\beta$ element of the pressure tensor. This gives six different viscosities. Each of the three directors can be perpendicular to the vorticity plane, and either of the two remaining directors can be perpendicular to the streamlines. If $\{\alpha, \beta, \gamma\}$ is an even permutation of $\{1, 2, 3\}$ the viscosity is denoted η_γ, and for odd permutations it is denoted $\eta_{-\gamma}$. The viscosities can be expressed in terms of time-correlation functions of the various elements of the pressure tensor [14].

$$\eta_1 = \eta_{2323;\,\Omega} + \gamma_{11;\,\Omega} + 2\eta_{231;\,\Omega} \tag{17}$$

$$\eta_{-1} = \eta_{2323;\,\Omega} + \gamma_{11;\,\Omega} - 2\eta_{231;\,\Omega} \tag{18}$$

$$\eta_2 = \eta_{3131;\,\Omega} + \gamma_{22;\,\Omega} + 2\eta_{312;\,\Omega} \tag{19}$$

$$\eta_{-2} = \eta_{3131;\,\Omega} + \gamma_{22;\,\Omega} - 2\eta_{312;\,\Omega} \tag{20}$$

$$\eta_3 = \eta_{1212;\,\Omega} + \gamma_{33;\,\Omega} + 2\eta_{123;\,\Omega} \tag{21}$$

and

$$\eta_{-3} = \eta_{1212;\,\Omega} + \gamma_{33;\,\Omega} - 2\eta_{123;\,\Omega} \tag{22}$$

We use a shorthand notation for the time correlation functions,

$$\eta_{\alpha\beta\gamma\delta;\,\Omega} \equiv \beta V \int_0^\infty ds \langle \mathring{p}^s_{\alpha\beta}(s)\, \mathring{p}^s_{\gamma\delta}(0) \rangle_{\mathrm{eq};\Omega} \tag{23}$$

$$\gamma_{\alpha\beta\gamma;\,\Omega} \equiv \beta V \int_0^\infty ds \langle p^a_\alpha(s)\, \mathring{p}^s_{\beta\gamma}(0) \rangle_{\mathrm{eq};\Omega} \tag{24}$$

$$\eta_{\alpha\beta\gamma;\,\Omega} \equiv \beta V \int_0^\infty ds \langle \mathring{p}^s_{\alpha\beta}(s)\, p^a_\gamma(0) \rangle_{\mathrm{eq};\Omega} \tag{25}$$

and

$$\gamma_{\alpha\alpha;\,\Omega} \equiv \beta V \int_0^\infty ds \langle p^a_\alpha(s)\, p^a_\alpha(0) \rangle_{\mathrm{eq};\Omega} \tag{26}$$

where

$$\mathring{p}^s_{\alpha\beta} = \tfrac{1}{2}(p_{\alpha\beta} + p_{\beta\alpha}) - \tfrac{1}{3}\, Tr(\mathbf{P})$$

is the symmetric traceless pressure and

$$p^a_\alpha = -\tfrac{1}{2}\, \varepsilon_{\alpha\beta\gamma} p_{\gamma\beta}$$

Table I. The Miesowicz Viscosities at a Reduced Density of 0.19 and a Reduced Temperature of 1.00

Viscosity	Estimate
η_1	9.7 ± 0.3
η_{-1}	0.57 ± 0.06
η_2	0.19 ± 0.005
η_{-2}	25 ± 3
η_3	4.9 ± 0.3
η_{-3}	0.59 ± 0.01

is the antisymmetric pressure. The subscript "eq" denotes an equilibrium ensemble. The subscript "eq: Ω" denotes an equilibrium ensemble where the constraint equation [Eq. (10)] is used to fix the directors. If $\alpha = \beta$ and $\gamma = \delta$, the correlation functions $\eta_{\alpha\beta\gamma\delta}$ are independent of whether the directors are fixed or not, i.e., the normal stress difference correlation functions are ensemble independent. The TCFIs involving the antisymmetric pressure are zero if the directors are free. Note that $\eta_{\alpha\beta\gamma;\,\Omega} = \gamma_{\gamma\alpha\beta;\,\Omega}$ because the pressure tensor is invariant under time reversal.

The various viscosities are given in Table I. We have $\eta_{-2} > \eta_1 > \eta_3 \gg \eta_{-3} \approx \eta_{-1} > \eta_2$. The ratio of the smallest and the largest viscosity coefficients is more than two orders of magnitude. The effective viscosity is

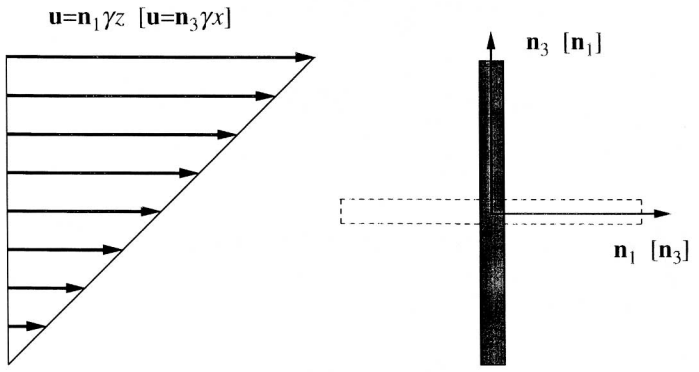

Fig. 3. Approximate orientation of the molecules when $\mathbf{n}_2$ is perpendicular to the vorticity plane. The symbols within square brackets pertain to the situation when $\mathbf{n}_3$ is parallel to the streamlines. The effective viscosity is then η_{-2}. The symbols outside the square brackets pertain to the case when $\mathbf{n}_1$ is parallel to the streamlines. The effective viscosity is then η_2.

consequently very orientation dependent. It is easy to realize that η_{-2} is the largest viscosity because this is the effective viscosity when $\mathbf{n}_1$ and thereby the $\hat{\mathbf{u}}_i$ axes are parallel to the streamlines and $\mathbf{n}_3$ and the $\hat{\mathbf{w}}_i$ axes are perpendicular to the shear plane (see Fig. 3). This means that it is very hard for the molecules to pass each other because their broadsides face the streamlines and hit each other. It is also easy to realize that η_2 is the smallest viscosity because in this orientation $\mathbf{n}_3$ and the $\hat{\mathbf{w}}_i$ axes are parallel to the streamlines and $\mathbf{n}_1$ and $\hat{\mathbf{u}}_i$ are perpendicular to the shear plane. This makes it very easy for the molecules to slide past each other, thus decreasing the viscosity.

5. CONCLUSION

We have devised a liquid crystal model potential consisting of nine oblate Gay–Berne interaction sites. Their axes of revolution are parallel to each other and perpendicular to the line joining the centers of mass. The length-to-breath-to-width ratio is 5:1:0.4. We have removed the attractive part of the Lennard–Jones core of the Gay–Berne potential and replaced it by a purely repulsive $1/r^{18}$ potential in order to reduce the number of interactions. This makes the system faster to simulate. This is useful when one wants to calculate transport properties which often require very long simulation runs to converge.

In order to generate an inertial director-based frame we use a director constraint algorithm that keeps the directors fixed an orthogonal. This constraint algorithm also generates a new equilibrium ensemble. Most time-correlation functions and thermodynamic properties are the same in this ensemble as in the conventional canonical ensemble. An important exception is the Green–Kubo relations for the viscosities. They are linear combinations of time-correlation-function integrals in the fixed-director ensemble, whereas they are complicated rational functions in the conventional canonical ensemble.

At high densities our liquid crystal model system forms a biaxial nematic phase. We have used the director-constraint algorithm to evaluate the Miesowicz viscosities of this phase. They can be regarded as the effective viscosities when one director is parallel to the streamlines, one director is perpendicular to the vorticity plane, and the last one is perpendicular to the shear plane. There are six such viscosities. They were found to be highly orientation dependent. The largest and the smallest viscosities differed by more than two orders of magnitude!

ACKNOWLEDGMENTS

The author gratefully acknowledges support of this research by the Swedish Natural Science Council (NFR) and the National Science

Foundation through Grant CTS-9101326. The computations on which the results in this work are based were performed on the Kendall Square parallel processor ofd the Oak Ridge National Laboratory in Oak Ridge, Tennessee.

REFERENCES

1. D. Baals and S. Hess, *Phys. Rev. Lett.* **57**:86 (1986); D. Baals and S. Hess, *Z. Naturforsch. Teil A* **43**:662 (1988).
2. D. Forster, *Ann. Phys.* **85**:505 (1974).
3. S. Sarman and D. J. Evans, *J. Chem. Phys.* **99**:9021 (1993).
4. J. G. Gay and B. J. Berne, *J. Chem. Phys.* **74**:3316 (1981).
5. S. Sarman, *J. Chem. Phys.* **103**:393 (1995).
6. S. Sarman, *J. Chem. Phys.* **105**:4211 (1996).
7. S. Sarman, *J. Chem. Phys.* **104**:342 (1996).
8. M. P. Allen, *Liq. Cryst.* **8**:499 (1990).
9. B. M. Mulder, *Liq. Cryst.* **1**:539 (1986).
10. D. J. Evans and G. P. Morriss, *Statistical Mechanics of Nonequilibrium Liquids* (Academic Press, London, 1990).
11. D. J. Evans, *Mol. Phys.* **80**:221 (1993).
12. J. H. Irving and J. G. Kirkwood, *J. Chem. Phys.* **18**:817 (1950).
13. S. Sarman and D. J. Evans, *J. Chem. Phys.* **99**:620 (1993).
14. S. Sarman, *J. Chem. Phys.* **107**:3144 (1997).